Modeling of Nonlinear Active Regions in TLM

Peter Russer, Poman P. M. So, and Wolfgang J. R. Hoefer

Abstract—**The modeling of active and nonlinear subregions of microwave structures using the transmission line matrix (TLM) method is discussed. It is shown that a correct modeling of subregions with negative conductivity is possible by lumped circuit elements connected to the TLM mesh nodes.**

I. Principle of Lumped Element Modeling

THE TRANSMISSION LINE matrix method, developed by Johns and Beurle [1] has emerged as a powerful method for computer modeling of electromagnetic fields [2], [3], and linear and nonlinear lumped element networks [4], [5]. Also the modeling of nonlinear passive subregions has already been treated [6]. It is well known that lossy subregions in TLM can be modeled by connecting a lumped resistor or an infinitely long transmission line stub across each mesh node [7]. While the resulting attenuation constant of the mesh is finite at low frequencies, it increases to infinity at the cutoff frequencies of the discrete network [2], [3]. Modeling regions with negative conductivity may yield uncontrollable instabilities at these frequencies. In reality, distributed active regions exhibit an intrinsic cutoff frequency. Correct TLM modeling must therefore include the real cutoff behavior in the discrete model, and the cutoff frequency of the TLM mesh must be sufficiently higher than the physical cutoff frequency of the real continuous active region.

We investigate initially the general case of a nonlinear admittance connected in parallel to a TLM shunt node. In general the relation between the node voltage $v(t)$ and the current $i(t)$ flowing into the nonlinear admittance will be governed by a nonlinear system of first order ordinary differential equations, if the nonlinear admittance can be modeled by lumped circuit elements. In the shunt TLM model, voltage wave amplitudes are used instead of voltage and current. We therefore substitute the voltage wave amplitudes $v_5^r(t) = [v(t) + i(t)/Y_r]/2$, and $v_5^i(t) = [v(t) - i(t)/Y_r]/2$ where $v_5^r(t)$ describes a voltage wave travelling from the TLM node toward the nonlinear admittance, and $v_5^i(t)$ describes a voltage wave incident from the nonlinear admittance on the TLM node. Y_r is the real characteristic admittance of the stub. Y_r may be chosen arbitrarily, however by an appropriate choice of Y_r calculations may be simplified. We consider the stub transmission line between the TLM node and the nonlinear admittance to be of infinitesimal length. This transmission line has no physical effect but ensures that by principle of causality the voltage wave reflected from the nonlinear admittance, $v_5^i(t)$, will be a nonlinear function of the voltage wave $v_5^r(t_,)$ incident on the nonlinear admittance with $t_1 \in (-\infty, t]$. We may model our lumped element network by a

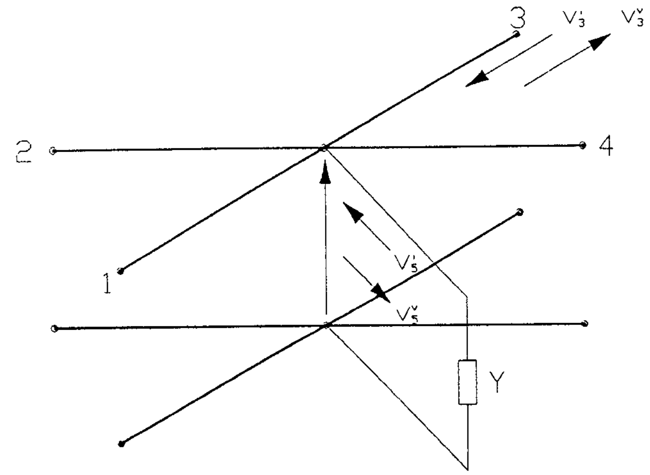

Fig. 1. Transmission line with voltage wave source parallel to TLM shunt node.

matched transmission line with characteristic admittance Y_r and an impressed voltage wave source $v_5^i(t)$ (see Fig. 1).

In the case of band limited signals, where all signals are completely determined by discrete sample values at time intervals Δt we may denote the time discrete description ${}_kV_5^r = v_5^r(k\Delta t)$, ${}_kV_5^i = v_5^i(k\Delta t)$. The scattering of impulses at a shunt mode loaded with a nonlinear admittance is described by

$$ {}_kV^r = S_k V^i, \tag{1}$$

where

$$ {}_kV^i = \left[{}_kV_1^i, {}_kV_2^i, {}_kV_3^i, {}_kV_4^i, {}_kV_5^i\right]^T, $$

and

$$ {}_kV^r = \left[{}_kV_1^r, {}_kV_2^r, {}_kV_3^r, {}_kV_4^r, {}_kV_5^r\right]^T $$

are the voltage wave vectors incident on and reflected from the node. The subscripts 1 to 5 refer to the branch numbers in Fig. 1. The characteristic impedance of the stub line connecting the node and the lumped load element may be chosen arbitrarily. We introduce the stub line characteristic admittance y_r normalized to the TLM mesh line characteristic admittance. Choosing $y_r = 4$, we can write (1) as

$$ {}_k\begin{bmatrix} V_1 \\ V_2 \\ V_3 \\ V_4 \\ V_5 \end{bmatrix}^r = \begin{pmatrix} -\frac{3}{4} & \frac{1}{4} & \frac{1}{4} & \frac{1}{4} & 1 \\ \frac{1}{4} & -\frac{3}{4} & \frac{1}{4} & \frac{1}{4} & 1 \\ \frac{1}{4} & \frac{1}{4} & -\frac{3}{4} & \frac{1}{4} & 1 \\ \frac{1}{4} & \frac{1}{4} & \frac{1}{4} & -\frac{3}{4} & 1 \\ \frac{1}{4} & \frac{1}{4} & \frac{1}{4} & \frac{1}{4} & 0 \end{pmatrix} {}_k\begin{bmatrix} V_1 \\ V_2 \\ V_3 \\ V_4 \\ V_5 \end{bmatrix}^i . \tag{2}$$

For $y_r = 4$ the matrix element S_{55} vanishes, and the voltage pulse ${}_kV_5^r$ scattered from the node to the load depends only on the voltage pulses ${}_kV_1^i$ to ${}_kV_4^i$ incident from the mesh lines and not on the voltage pulse ${}_kV_5^r$ incident from the load element on

Manuscript received September 28, 1990. This work was supported by the Deutsche Forschungsgemeinschaft.

P. Russer is with the Lehrstuhl für Hochfrequenztechnik,Technische Universität München,Arcisstrasse 21, D-8000 Munich 2, Germany.

P. P. M. So and W. J. R. Hoefer are with the Laboratory of Electromagnetics and Microwaves, Department of Electrical Engineering, University of Ottawa, Ottawa, ON, K1N 6N5 Canada.

IEEE Log Number 9041182.

1051-8207/91/0100-0010$01.00

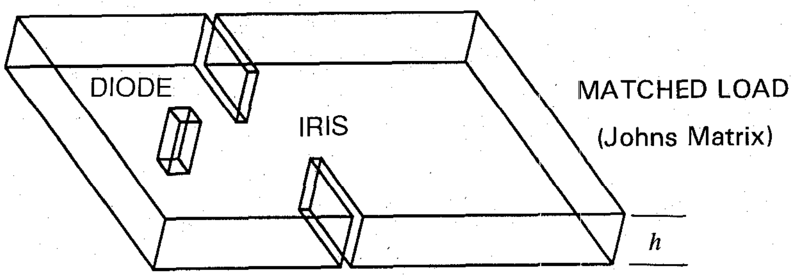

Fig. 2. Layout of TLM grid of diode oscillator.

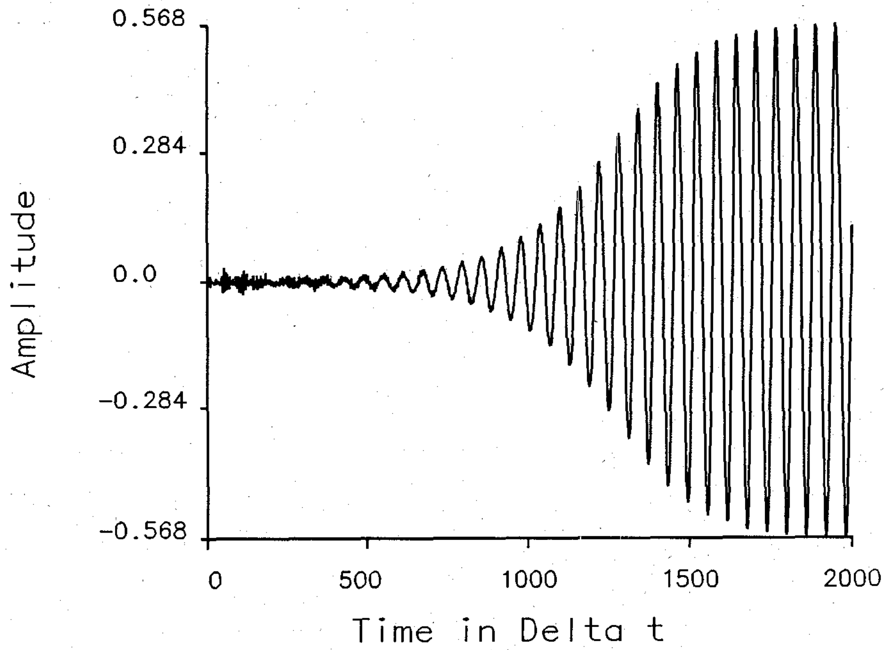

Fig. 3. Time evolution of oscillator output waveform.

the mesh node. Therefore ${}_kV_5^r$ may be computed directly from the incident voltage pulses without solving a nonlinear equation. The voltage wave pulses ${}_kV_n^i(z, x)$ incident on a TLM mesh node depend on the voltage wave pulses ${}_{k-1}V_n^r(z_1, x_1)$ emerging from the neighbouring nodes as follows:

$$\begin{aligned} {}_{k+1}V_1^i(z, x) &= {}_kV_3^r(z, x-1) \\ {}_{k+1}V_2^i(z, x) &= {}_kV_4^r(z-1, x) \\ {}_{k+1}V_3^i(z, x) &= {}_kV_1^r(z, x+1) \\ {}_{k+1}V_4^i(z, x) &= {}_kV_2^r(z+1, x). \end{aligned} \tag{3}$$

II. Modeling of an Active Diode

As an example we discuss a simple active diode model with an intrinsic cutoff frequency. The equivalent circuit comprises a nonlinear conductance $G(v_1)$, a linear series resistor R, and a linear parallel capacitor C. The diode is assumed to have a region of negative differential conductance. The diode is distributed over a number N of TLM mesh nodes. We must thus connect to each of these mesh nodes the diode model with all impedances multiplied by N and all admittances divided by N. The network equations for the equivalent diode circuit, scaled by N are $v - v_1 = NRi$, $i - i_1 = \frac{1}{N}C\frac{dv_1}{dt}$, and $i_1 = \frac{1}{N}f(v_1)$.

Expressing $v(t)$ and $i(t)$ by $v_5^r(t)$ and $v_5^i(t)$ we obtain

$$\frac{du(t)}{dt} + \frac{1}{\tau}g(u(t)) = \frac{1-\Gamma_R}{\tau}v_5^r(t) \tag{4}$$

with the variable $u(t) = v_5^i(t) - \Gamma_R v_5^r(t)$, the time constant $\tau = \left(R + \frac{1}{NY_r}\right)C$, the reflection coefficient $\Gamma_R = \frac{NRY_r - 1}{NRY_r + 1}$, and the function $g(u) = u + \frac{1}{NY_r}f((1 + NRY_r)u)$. Equation (4) can be integrated numerically using the same time step Δt as the TLM field simulation in the propagation space adjacent to the diode. We introduce the nonlinear conductance $G(v_1)$ by $f(v_1) = v_1G(v_1)$ and assume that $G(v_1)$ varies only slowly from one time step to the next, so that its value can be taken from the previous iteration. The discretized formulation of (4) is then

$${}_kV_5^i = \frac{{}_{k-1}\alpha_k v_5^r + {}_{k-1}v_5^i - \Gamma_R\, {}_{k-1}v_5^r}{{}_{k-1}\beta} \tag{5}$$

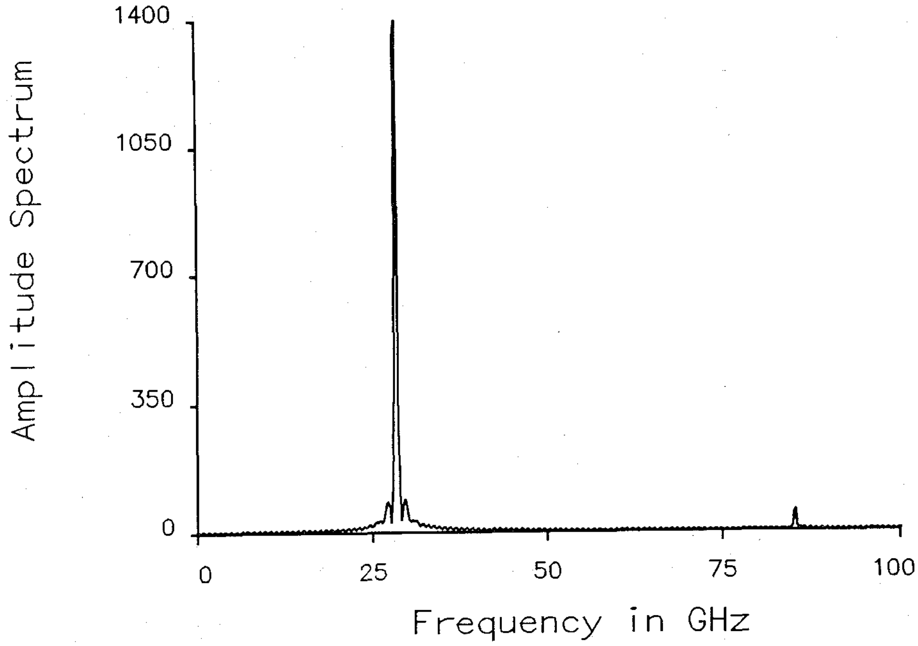

Fig. 4. Output spectrum of oscillator in steady state.

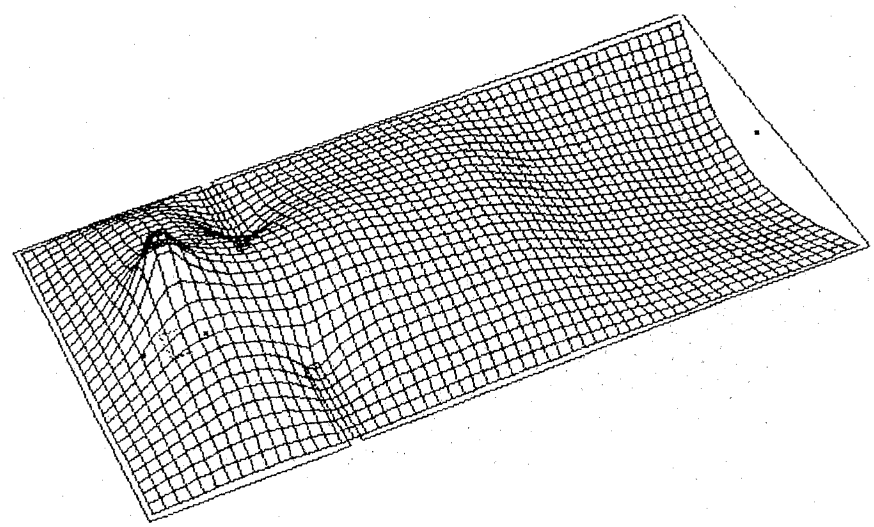

Fig. 5. Two-dimensional field distribution in oscillator.

with

$$ {}_{k-1}\alpha = \Gamma_R + \frac{\Delta t}{\tau}\left[1 + \left(R - \frac{1}{NY_r}\right)G\left({}_{k-1}V_1\right)\right] \quad (6)$$

$$ {}_{k-1}\beta = 1 + \frac{\Delta t}{\tau}\left[1 + \left(R + \frac{1}{NY_r}\right)G\left({}_{k-1}V_1\right)\right] \quad (7)$$

$$ {}_{k-1}V_1 = {}_{k-1}V_5^r + {}_{k-1}V_5^i - NRY_r\left({}_{k-1}V_5^r - {}_{k-1}V_5^i\right). \quad (8)$$

The time step is $\Delta t = \Delta l / c$, where Δl is the TLM mesh width, and c is the wave velocity on the TLM lines.

III. A Diode Oscillator

We have implemented the above algorithm and investigated the time evolution of the field in a planar diode oscillator. For the active diode a simple model was chosen with the nonlinear conductance described by the cubic polynomial voltage current characteristic

$$ f(v_1) = G(v_1)v_1 = -\left|G_{1\max}\right|\left[1 - \frac{1}{3}\left(\frac{v_1}{v_m}\right)^2\right]v_1. \quad (9)$$

The differential conductivity $-\left|G_{1\max}\right|\left[1 - \left(\frac{v_1}{v_m}\right)^2\right]$ is negative for $v_1 \in (-v_m, v_m)$. The maximum negative slope is $-\left|G_{1\max}\right|$ for $v_1 = 0$.

Fig. 2 shows the geometry of the oscillator in a reduced height WR-28 waveguide. All sidewalls and the inductive iris are electric walls, while the long output waveguide section is terminated in a wideband matched load (Johns matrix wall). The diode is centered in the rectangular resonator.

The following figures have been obtained by TLM simulation for the following diode characteristics: $R = 4\Omega$, $C = 0.07pF$, $G_{1\max} = -4mS$. The diode is distributed over an area of $6\Delta l^2$

and the height of the planar structure is $h = 0.5$ mm. The corresponding characteristic admittance of the 2D-TLM mesh lines must be $Y_0 = \Delta l/(\sqrt{2}\,\eta_0 h = 0.92\ mS$, and hence $Y_r = 4Y_0 = 3.68\ mS$. The air-filled resonator measures $29\,\Delta l$ in width and $16\,\Delta l$ in length, with $\Delta l = 0.2452$ mm. The iris walls are Δl thick and $13\,\Delta l$ wide. Figs. 3–5 show the behavior of the oscillator model. The oscillation builds up exponentially from the noise injected into the mesh to start the process (see Fig. 3). The amplitude then saturates when the nonlinear conductance is driven into positive values. The steady-state waveform reveals the presence of a third harmonic that is also clearly visible in the spectrum of the output signal (see Fig. 4). Due to the low cutoff frequency of the diode ($f_c = 71$ GHz), the third harmonic is 20 dB below the fundamental wave. No oscillations at the TLM mesh cutoff frequency ($f_{cM} = 306$ GHz) have been observed, which indicates, that instabilities at this frequency have clearly been suppressed through the inclusion of the diode capacitance in the algorithm. The field distribution in Fig. 5 demonstrates the interaction between the diode and the structure.

IV. Conclusion

A TLM method for modeling distributed circuits containing nonlinear active elements and structures was demonstrated. The scattering properties of the nonlinear element are expressed in terms of its differential equations that are solved by stepwise integration with the time step of the TLM algorithm. A cavity oscillator with an active diode with a finite cutoff frequency has been modeled. Spurious oscillations of the TLM mesh that regularly occur when including negative conductivity or pulse reflection coefficients larger than unity were effectively suppressed.

Acknowledgment

The authors wish to thank to Mr. B. Isele and to Dr. R. Weigel for a critical reading of the letter.

References

[1] P. B. Johns and R. L. Beurle, "Numerical solution of two-dimensional scattering problems using a transmission-line matrix," *Proc. IEE*, vol. 118, no. 9, pp. 1203–1208, Sept. 1971.

[2] W. J. R. Hoefer, "The transmission line matrix method—theory and applications," *IEEE Trans. Microwave Theory Tech.*, vol. MTT-33, no. 10, pp. 882–893, Oct. 1985.

[3] —, "The transmission line matrix (TLM) method," in *Numerical Techniques for Microwave and Millimeter Wave Passive Structures*, Chapter 8, T. Itoh, Ed. New York: John Wiley, 1989, pp. 496–591.

[4] J. W. Bandler, P. B. Johnes, and R. H. Rizk, "Transmission-line modeling and sensitivity evaluation of lumped network simulation in the time domain," *J. Franklin Inst.*, vol. 304, pp. 15–23, 1977.

[5] P. B. Johns and M. O'Brien, "Use of the transmission line modeling (T.L.M.) method to solve nonlinear lumped networks," *Radio Electron. Engineer*, vol. 50, no. 1/2, pp. 59–70, Jan./Feb. 1980.

[6] S. A. Kosmopoulos, W. J. R. Hoefer, and A. Gagnon, "Non-linear TLM modeling of high-frequency varactor multipliers and halvers," *Int. J. Infrared Millimeter Waves*, vol. 10, no. 3, pp. 343–352, Mar. 1989.

[7] S. Akhtarzad, "Analysis of lossy microstrip structures and microstrip resonators by the TLM method," Ph.D. dissertation, Univ. of Nottingham, England, July 1975.